# Structural transitions and dipole moment of water clusters $(H_2O)_{n=4-100}$

Julián Gelman-Constantin,[1] Marcelo A. Carignano,[2,a)] Igal Szleifer,[2] Ernesto J. Marceca,[1] and Horacio R. Corti[1,3]
[1]*Instituto de Química Física de los Materiales, Medio Ambiente y Energía (INQUIMAE), Facultad de Ciencias Exactas y Naturales, Universidad de Buenos Aires, Pabellón II, Ciudad Universitaria, C1428EGA Buenos Aires, Argentina*
[2]*Department of Biomedical Engineering and Chemistry of Life Processes Institute, Northwestern University, 2145 Sheridan Rd., Evanston, Illinois 60208, USA*
[3]*Departamento de Física de Materia Condensada, Centro Atómico Constituyentes, Comisión Nacional de Energía Atómica (CNEA), San Martín, B1650KNA Buenos Aires, Argentina*

(Received 6 April 2010; accepted 31 May 2010; published online 14 July 2010)

The properties of water clusters $(H_2O)_n$ over a broad range of sizes (n=4–100) were studied by microcanonical parallel tempering Monte Carlo and replica exchange molecular dynamics simulations at temperatures between 20 and 300 K, with special emphasis in the understanding of relation between the structural transitions and dipole behavior. The effect of the water interaction potential was analyzed using six nonpolarizable models, but more extensive calculations were performed using the TIP4P-ice water model. We find that, in general, the dipole moment of the cluster increases significantly as the cluster melts, suggesting that it could be used to discriminate between the solidlike and liquidlike phases. The effect of a moderate electric field on the cluster heat capacity and total dipole moment was found to be negligible. © *2010 American Institute of Physics*. [doi:10.1063/1.3455716]

## I. INTRODUCTION

The properties of water clusters are fundamental for understanding water in biological systems[1] and in atmospheric chemistry[2,3] since they play an important role as a link between the single water molecule and the behavior of liquid and nanoconfined water. The evolution of some dynamic and thermodynamic properties from small clusters to bulk water could be the key, for instance, to elucidate the nature of the deep supercooled water behavior[4,5] or to describe the several amorphous (glassy) water, which can be derived from vapor, liquid, or solid water.[6] In this study, we explore the viability of characterizing the structure of a given cluster using as a signature the magnitude of its dipole moment, and consider the use of this property as a tool to monitor phase changes in nanoscale.

The possibility of having experimental access to the overall dipole moment of small water clusters motivated several studies in the past years.[7–12] Early electric focusing experiments[7] performed on a beam of clusters $(H_2O)_n$, with $2 \leq n \leq 17$, showed that except for the dimer, the rest of the aggregates do not exhibit polar behavior, suggesting that they form cyclic, closed ring structures. However, by use of terahertz laser vibration-rotation tunneling spectroscopy, Saykally and co-workers[10] showed conclusively that the most stable structure for $(H_2O)_6$ is polar ($\mu \approx 2$ D) and corresponds to a so-called cage configuration. The apparent paradox was analyzed by Rodriguez *et al.*[13] and they were able to reconcile the results by considering the effect of temperature on the resulting dipole moment of the clusters. The dipole moment was also investigated by electron deflection (ED) experiments on a highly collimated beam of water clusters with $3 \leq n \leq 18$,[14] revealing a small paraelectric response originated in the effective (electronic+orientational) polarizability of the clusters. By considering that the instantaneous global dipole partially orients along the electric field's axis according to a canonical distribution, the authors gave a procedure to estimate the vibration-averaged dipole moments of the clusters from the measured effective polarizabilities and the calculated electronic polarizabilities. The dipole moment of all the clusters was found to be slightly larger than 1 D, displaying a small increase with the cluster size. Unfortunately, the interpretation of these results is obscured by the difficulty in assigning temperatures to the water clusters generated in nonequilibrium conditions.

There is a lack of dipole moment calculations for clusters using computer simulations, especially as a function of the cluster's temperature. Two studies address the relation between the structure of the cluster and its dipole moment using polarizable water models.[15,16] However, these studies consider the optimized structures and/or clusters at 298 K. In this paper we use microcanonical parallel tempering Monte Carlo (mPTMC) and replica exchange molecular dynamics (REMD) simulations to study the relation between the structure and dipole moment of water clusters as a function of temperature. We consider clusters with $4 \leq n \leq 20$ with six nonpolarizable water models, including the TIP4P-ice (Ref. 17) water model that, as far as we know, has been considered only for clusters with n=20.[18] It is important to mention here that the parameters of the TIP4P-ice model have been fitted to the melting and coexistence lines involving different ice phases without deterioration of the rest of the properties. Consequently it reproduces well the phase diagram of water

a)Electronic mail: cari@northwestern.edu.

 

(especially at moderated pressures) and it is expected to be an excellent model in studies of equilibrium water structures. For the TIP4P-ice model we extend our study to large clusters using mPTMC ($4 \leq n \leq 80$) and MD ($40 \leq n \leq 100$). In all cases, our calculation is limited to the orientational (conformational) contribution of the dipole moment since nonpolarizable models are used.

This paper is organized in the following way: in Sec. II we briefly describe the water models used and the computer simulations methods. In Sec. III we present the results for the structural transitions and dipole moment as a function of temperature, and a final summary and conclusion are presented in Sec. IV

## II. MODELS AND METHODS

We studied water clusters $(H_2O)_n$, with $4 \leq n \leq 100$, using six different nonpolarizable water models: simple point charge (SPC),[19] simple point charge/extended (SPC/E),[20] TIP3P (Ref. 21) (three-sites models), TIP4P,[22] TIP4P-ice (Ref. 17) (four-sites models), and TIP5P (Ref. 23) (five-sites model). The electric dipolar moments and bulk melting temperatures for these models are summarized in Table I.

TABLE I. Electric dipolar moment of the isolated molecule and bulk melting temperature for the six classical models tested in this work.

| Model | $\mu$ (D) | $T_m$ (K)[a] |
|---|---|---|
| SPC | 2.274 | 190.5 |
| SPC/E | 2.351 | 215.0 |
| TIP3P | 2.347 | 146.0 |
| TIP4P | 2.177 | 232.0 |
| TIP4P-ice | 2.426 | 272.2 |
| TIP5P | 2.292 | 273.9 |

[a]$T_m$ from Ref. 24, except for the TIP4P-ice model, taken from Ref. 17.

In the proximity of a phase transition, a system may show a break in ergodicity. This implies that a simple Metropolis algorithm would not be appropriate in such a case. The approach that we followed to overcome this problem consists in using the parallel tempering method.[25,26]

In a parallel tempering Monte Carlo (MC) scheme, several simulations at different temperatures are performed simultaneously, and each one is allowed to evolve according to the Metropolis algorithm. For the present study we have used an implementation of the *microcanonical* ensemble to MC simulations based on the work of Pearson *et al.*,[27] as done previously.[28] At a regular frequency, a swap between the configurations of systems with neighboring energies is attempted and the acceptance probability of the swaps is calculated as

$$P = \min\left(1, \frac{[E_i - U(x_j)]^{F/2-1}[E_j - U(x_i)]^{F/2-1}\Theta(E_i - U(x_j))\Theta(E_j - U(x_i))}{[E_i - U(x_i)]^{F/2-1}[E_j - U(x_j)]^{F/2-1}}\right), \quad (1)$$

where $E$ is the total energy of the box, $U$ is its potential energy, and $F$ is the total number of degrees of freedom of the system, which for a system of n rigid molecules corresponds to 6n. The Heaviside step function, $\Theta(E\text{-}U)$, allows only the configurations with positive kinetic energy. This "unphysical" move lets the system surpass potential energy barriers. Hence, it is necessary that at least one simulation box has a total energy high enough to jump all the energy barriers. It has been shown that this combination satisfies both ergodicity and detailed balance.[26]

An in-house developed program was used. The cluster is placed in a spherical cavity to avoid the loss of molecules by evaporation. The radius of the cavity, which only has moderate effect on the determination of the melting temperature,[18] was set to R=1.0 nm for the smaller systems (n=4, 6, and 8) and gradually increased to R=2.0 nm for the larger systems (n=40, 60, and 80). The intermediate values are R=1.2 nm (n=9, 10, 11, and 12), R=1.3 nm (n=13 and 14), R=1.4 nm (n=16), and R=1.5 nm (n=20). Depending on the case, between 20 and 32 simulation boxes were used, with total energies corresponding to temperatures from 20 to 300 K, approximately. The systems were allowed to equilibrate for $(10-70)\times 10^6$ MC steps and then runs of $(20-50)\times 10^6$ MC steps were used to compute the average of the magnitudes of interest. For n=40, longer runs of $750\times 10^6$ MC steps were performed, in order to compare with the behavior of equally long simulations in the presence of an external electric field. The swaps between configurations were attempted once every 500–10 000 MC steps. Here we refer to MC steps as one attempt to translate and rotate every molecule in the system.

The electric dipolar moment was calculated following the classical definition:

$$\mu = \sum_i x_i q_i, \quad (2)$$

where the index $i$ runs over all the charges present in the system and $x_i$ is the position vector of the charge $q_i$.

REMD simulations were performed using GROMACS 3.3.2.[29,30] The cluster is placed in a cubic box with periodic boundary conditions (pbc). The size of the box is sufficiently large so that no molecule in the cluster sees any part of the periodic image of the cluster. As a result of the pbc there is no evaporation of water molecules outside of the simulation box. The dimension of the simulation box was 3.0 nm for the clusters with n=40, 60, and 80 molecules, and 5.0 nm for the cluster of 100 water molecules. The number of replicas used in the simulations was 24 for the smaller systems (n=40, 60, and 80) with temperatures between 30 and 300 K. For the

largest cluster (n=100) 40 replicas with temperature from 6 to 300 K were employed.

The integration was done using the leap-frog algorithm, with a time step of 1 fs. The temperature of the individual boxes was kept constant with a Nosé–Hoover algorithm, and the SHAKE algorithm was used in order to maintain the intramolecular distances and angles. The REMD scheme is analog to the parallel tempering scheme in MC. Several boxes at different temperatures ("replicas") are run simultaneously, and a swap between replicas of neighboring temperatures is attempted regularly. We used between 24 and 40 replicas, and a swap attempt every 100–1000 ps. The length of the simulations was usually of 10 ns, but longer runs (500 ns) were performed for the largest clusters.

## III. RESULTS AND DISCUSSION

One of the characteristics of clusters is that solid and liquid forms can coexist in an ensemble over a range of energies or temperatures.[31] The transitions between solidlike and liquidlike structures, as those observed in this work and in previous ones, are commonly referred to as a *melting transition* in the cluster literature. However these transitions should not be considered as thermodynamic phase transition, a concept strictly valid for macroscopic systems.

In some particular cases, as occur for water clusters with n=8 and n=12, the transitions are associated with sharp peaks in the heat capacity ($C_v$), with the corresponding steep jumps in energy. In other cases of small and medium clusters, the transition has been associated to isomerizations rather than to a solid to liquid phase change. Namely, as the temperature increases the cluster has several rigid structures that are energetically accessible, but the transition between them (if occurs) is a sudden transition between solidlike structures. A further increase of the temperature is needed to melt the cluster to the liquidlike state where the structural changes happen in a continuous manner. Large clusters also exhibit $C_v$ changes that are usually weak and span a wide temperature range, presumably due to a gradual melting starting at the cluster's surface. In some cases the transition could also be associated with the kinetically defined glass transition, that is, the conversion of an amorphous solid into a supercooled liquid as temperature increases.

In Fig. 1(a) we compare the $C_v$ shapes of transitions observed in mPTMC simulations for clusters with n=8, 13, and 80 using the TIP4P-ice model, where the main characteristics of the small, medium, and large clusters mentioned above are displayed. The corresponding cluster average dipole moments ($\langle|\mu|\rangle$, per molecule) are displayed in Fig. 1(b). For the smaller clusters, there is a clear relation between the properties: As the cluster melts, the average dipole moment increases. For the largest cluster the melting transition is displayed by a weak increase in $C_v$ that corresponds to a weak increase in the average dipole moment.

The behavior of $C_v$ in the small $T$ limit depends whether the interactions are treated with classical or a quantum theory.[32,33] In the present work we have no intention of treating this limit and our approach is completely classical, which is inconsistent with the zero temperature limit. There are

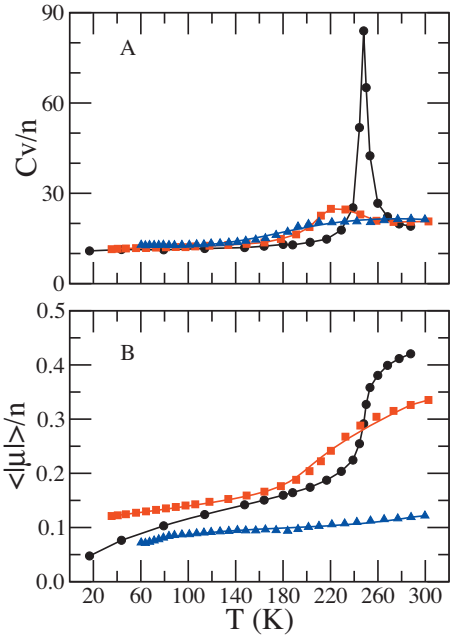


FIG. 1. (a) Heat capacity (cal $K^{-1}$ $mol^{-1}$) and (b) dipole moment (D) as a function of temperature obtained with the TIP4P-ice model for water clusters with n=8 (black circles), n=13 (red squares), and n=80 (blue triangles).

studies that have properly included the quantum degree of freedom in order to understand the low temperature limit, see Refs. 32–35.

The solid-liquid transition in water clusters was studied by many authors for different cluster sizes. However, the use of different simulation techniques, limited cluster sizes, and mainly, different intermolecular potentials prevented to formulate a general conclusion on the effect of size. As an example of the effect of the intermolecular potential, we show in Fig. 2(a) the heat capacity of the water octamer as a function of temperature for the six water model that we consider. In all cases there is a well defined transition, with peaks in the $C_v$ curves at temperatures between 120 K (TIP3P) up to 248 K (TIP4P-ice), depending on the model. As displayed by the $C_v$ curves, the sharper transitions correspond to the TIP4P and TIP4P-ice models, while the TIP3P potential exhibits the broadest transition. The strong dependency of $T_m$ with the water model for the octamer agrees with previous studies using MC techniques.[28,36–38] At temperatures below the transition temperature, the dominant structures for the octamer, regardless of the model, are the cubic $S_4$ and $D_{2d}$ structures already described by Tsai and Jordan[36] for TIP3P water, Nigra *et al.*[39] for MCY (Matsuoka–Clementi–Yoshimine) water, and Rodriguez *et al.*[13] in MCY and TIP4P water. At temperatures above melting more open and disordered structures are observed. The corresponding changes in the cluster dipole moment for the different models are displayed in Fig. 2(b). In spite of the different transition temperatures, the values of the dipole moments corresponding to the solid and liquid states are consistent across the models. Moreover, the dipole moment of clusters calculated with density functional calculations produces results quantitatively similar to those obtained with one of the molecular models used in this paper.[40]

A comprehensive summary of the findings of previous

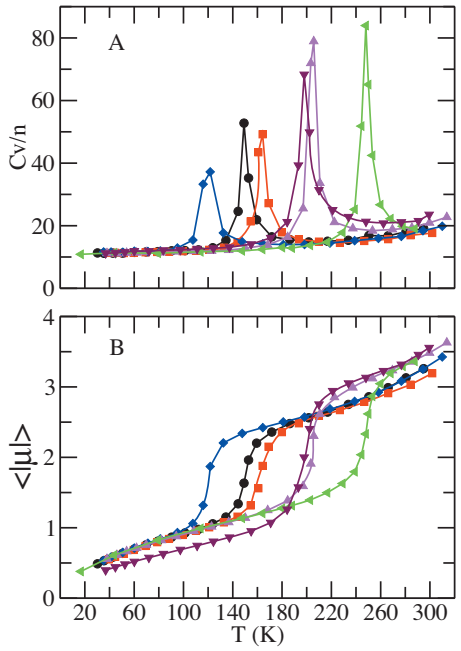


FIG. 2. (a) Heat capacity (cal $K^{-1}$ $mol^{-1}$) and (b) dipole moment (D) as a function of temperature for the water octamer. Different colors correspond to different water models: SPC (black circles), SPC/E (red squares), TIP3P (blue diamonds), TIP4P (magenta up-triangles), TIP4P-ice (green left-triangles), and TIP5P (maroon down-triangles).

simulation works using a variety of water models was recently compiled by Egorov[41] (see Table I of Ref. 41). In this work we analyzed $(H_2O)_n$ clusters with n=8,12,16,20 using the six water models mentioned above. Additionally, we studied clusters with n=4, 6, 9, 10, 11, 13, 14, 40, 60, 80, and 100 using the TIP4P-ice potential, which remains untested [except for n=20 (Ref. 18)] in the abundant literature on water clusters. As indicator of the melting transition we monitor $C_v$ as a function of the temperature. The $C_v$ criterion consists in taking the temperature of the peak or, if there is a jump instead of a peak, the temperature of the inflexion point. We concentrate our attention in the effect of the melting on the cluster dipole moment and we analyze this property as an indicator of the melting transition. Whenever possible, we calculate the melting temperature from the curve of dipole moment versus temperature, where the inflexion point of the jump or change of slope was taken as the transition temperature. Table II summarizes our results for the transition temperatures obtained in our mPTMC and REMD simulations with the different water models.

For the particular case of the TIP4P-ice model, we show in Fig. 3 the $C_v$ curves for all the simulated clusters. On the top panel we grouped all the cases where the melting transition is well defined, and the bottom panel shows the other cases where the $C_v$ curve has less structure. No particular signal of a melting transition was observed for the TIP4P-ice tetramer, contrasting with the reported results for the TIP5P and the CKL (Cieplak–Kollman–Lybrand) models by Carignano[28] and by Vegiri and Farantos,[42] respectively. However, a weak and broad transition was detected from the heat capacity curve of the hexamer. Jordan *et al.*[37,38] also observed a weak $C_v$ peak for the hexamer at T≈90 K (T≈60 K) for the TIP4P and NCC (Niesar–Corongiu–Clementi) [DC (Dang–Chang) and MCY] models. Other models (such as the SPC/E) do not show a $C_v$ peak. From n=8 to n=11 the clusters display an evolution from a sharp transition to weaker or continuous one. Thus, the transition for n=9 is less sharp than that of the octamer, but still well defined in agreement with previous findings for the TIP4P model.[38] For n=10 the $C_v$ peak is broad and weak and for n=11 the $C_v$ does not exhibit a peak, but a smooth increase with increasing temperature. The n=12 cluster displays the sharp transition like that of the octamer, also model-dependent (see Table II). There is no reported $C_v$ behavior for the dodecamer in literature, although Adeagbo and Entel[43] found a well defined jump in the caloric curve for this cluster as compared to the n=10 and n=15 clusters, and reported $T_m$=205 K using the TIP4P potential. The melting temperature determined by Egorov *et al.*[41] by MD for this potential is much lower, $T_m$=134 K. Our result for the transition temperature of the dodecamer with the TIP4P potential is in between the above mentioned values.

The transitions for n=13 and n=14 are weaker than that

TABLE II. Transition temperatures of water clusters obtained from the mPTMC and MD simulations.

| | | mPTMC | | REM |
|---|---|---|---|---|
| *n* | Model | $C_v$ | $\langle\|\mu\|\rangle$ | $C_v$ |
| 6 | TIP4P-ice | 116 | 124 | |
| 8 | SPC | 150 | 150 | |
| | SPC/E | 163 | 163 | |
| | TIP3P | 123 | 122 | |
| | TIP4P | 202 | 202 | |
| | TIP5P | 199 | 197 | |
| | TIP4P-ice | 248 | 248 | |
| 9 | TIP4P-ice | 246 | 240 | |
| 10 | TIP4P-ice | 189 | 186 | |
| 11 | TIP4P-ice | 216 | ··· | |
| 12 | SPC | 114 | 112 | |
| | SPC/E | 123 | 123 | |
| | TIP3P | 97 | 103 | |
| | TIP4P | 175 | 174 | |
| | TIP5P | 202 | 198 | |
| | TIP4P-ice | 214 | 213 | |
| 13 | TIP4P-ice | 227 | 217 | |
| 14 | TIP4P-ice | 225 | 228 | |
| 16 | SPC | 123 | 123 | |
| | SPC/E | 137 | 136 | |
| | TIP3P | 120 | 121 | |
| | TIP4P | 137 | 140 | |
| | TIP5P | 174 | 160 | |
| | TIP4P-ice | 153 | 165 | |
| 20 | SPC | 126 | 141 | |
| | SPC/E | 130 | 136 | |
| | TIP3P | 116 | 115 | |
| | TIP4P | 142 | 142 | |
| | TIP5P | 173 | 175 | |
| | TIP4P-ice | 155 | 162 | |
| 40 | TIP4P-ice | 161 | 169 | 167 |
| 60 | TIP4P-ice | 174 | 160 | 175 |
| 80 | TIP4P-ice | 180 | 170 | 168 |
| 100 | TIP4P-ice | | | 170 |

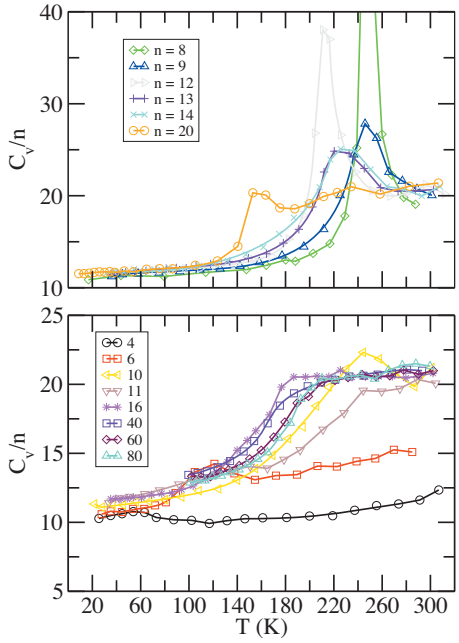


FIG. 3. Heat capacity (cal $K^{-1}$ $mol^{-1}$) for TIP4P-ice $(H_2O)_n$ clusters. On the top panel we grouped the clusters with well defined melting transition, while weaker transitions are represented in the bottom panel.

corresponding to the dodecamer, but still well defined. For n=16 the $C_v$ curve shows a monotonic increase until it reaches a plateau. For n=20, there is a clear peak although it occurs at a lower temperature than that of the smaller clusters ($T_m$=155 K), and in close agreement with the results of Douady *et al.*[18]

For large clusters, with n=40, 60, and 80 the observed $C_v$ curves correspond to weak transitions. There are few MC studies for large clusters (n>20). Shevkunov and Vegiri[44,45] studied water cluster, with n=40 and n=64, by means of MC simulations with the four charges ST2 potential. The $C_v$ curves reported by these authors for both clusters show a weak peak before reaching a plateau close to the peak value, a pattern quite similar to that observed for our simulation for n=20. The melting temperatures assigned by Shevkunov and Vegiri for the clusters n=40 and n=64 are 208 and 210 K, respectively, which are higher than those found in our simulations (Table II) for n=40 and n=60 with the TIP4P-ice potential

Figure 4 summarizes our results for the melting tempera-

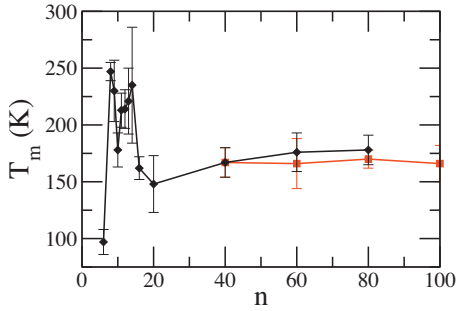


FIG. 4. Melting temperatures of water cluster calculated by PTMC (black rhombuses) and REMD (red squares) from the $C_v$ curves for TIP4P-ice model. Error bars represent an estimate of the width of the transition.

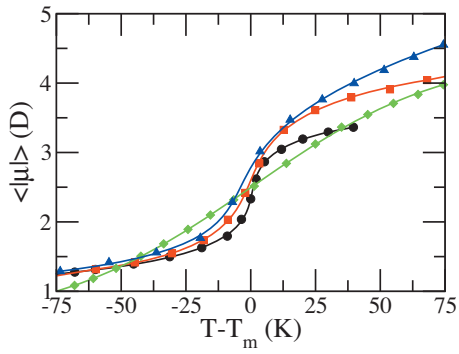


FIG. 5. Total dipole moment of TIP4P-ice water clusters with n=8 (black circles), n=12 (red squares), n=16 (green diamonds), and n=20 (blue triangles).

ture for TIP4P-ice. We observed high transition temperatures with fluctuations for clusters with $8 \leq n \leq 14$ due to the stability of the structures formed. These fluctuations are not observed, neither for our results for TIP4P nor for the results of Egorov *et al.*[41,46,47] using the same model because only the more stable clusters (n=8, 12, 16, and 20) were studied. The presence of structural "magic numbers" in atomic and molecular clusters has been discussed previously.[39] The transition temperature becomes a slightly but steadily increasing function of the size for $n \geq 20$, with values between 160 and 180 K for the largest clusters.

These mPTMC and MD transition temperatures using the TIP4P-ice model may raise the question whether the transitions in the largest clusters are analogous to solid-liquid transitions in macroscopic systems or they are related to glass transitions. Experimental evidence by Torchet *et al.*[48] showed that clusters with n<200 were amorphous at temperatures around 180±20 K. Contrarily, the MD results[41] with the TIP4P model predict that clusters of that size would be liquid.

The reported glass transition temperature of bulk water, (136±1) K, is based on thermal analysis of amorphous solid water[49,50] and hyperquenched water,[51–53] but this value was questioned by Angell and co-workers,[54] who argued that it could be around (165±5) K, as the true glass transition temperature of annealed amorphous water. Whether the transition temperatures observed in these large, but still nanoscopic, clusters are an indication of a glass to liquid transition it requires, however, more detailed studies.

It has been argued that large clusters ($n \geq 90$) have a configurational energy similar to that of ice cuts of equal size.[55] The question that arises is as follows: What is the melting temperature of ice particles of similar size and how this temperature compares with the melting of optimal clusters? This problem, which is related to the Gibbs–Thomson effect,[56] is beyond the scope of this work and it will be investigated in the near future.

Figures 5 show the total dipole moment of TIP4P-ice clusters with n=8, 12, 16, and 20 as a function of the temperature, relative to the corresponding transition temperature. The general behavior corresponds to a substantial increment of this quantity with the temperature, exhibiting a sharp change at the transition temperature. This pattern is observed

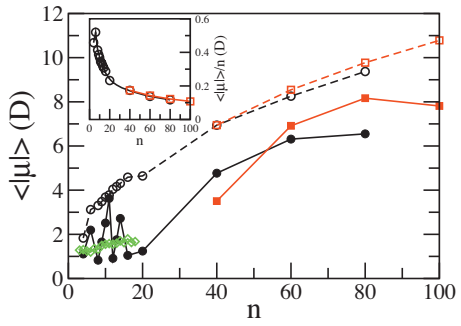


FIG. 6. Total dipole moment of water clusters obtained with mPTMC (black circles) and MD simulations (red squares) for the TIP4P-ice model at low (solid symbols) and high (open symbols) temperatures. The experimental results by Moro *et al.* (Ref. 14) are presented for comparison (green rhombuses). The inset shows the dipole moment per molecule in the high temperature regime.

for the SPC, SPC/E, TIP4P, and TIP4P-ice water models, while the TIP3P and TIP5P models present some anomalous behavior, particularly at low temperature (solidlike region). For all studied sizes, the TIP4P-ice model yields the higher total dipole moment at high temperature. TIP4P gives results similar to TIP4P-ice for $8 \leq n \leq 16$. In the liquidlike region, SPC, SPC/E, and TIP3P models render almost identical results within this size range, being the temperature dependence weaker for n=16.

For T=280 K, the highest temperature considered in this study, the total dipole moment increases monotonously with the cluster size for all the models. In these conditions, model-dependent differences in the calculated dipole moments never exceed 0.3 D, and in all cases TIP4P, TIP5P, and TIP4P-ice models give the larger values while SPC/E leads to the lower ones.

The temperature behavior of the dipole moment of the clusters can be understood by analyzing their structure before and after the transition. At low temperatures, clusters adopt (especially for the smaller sizes) well-ordered rigid structures that in average, present small dipole moments due to the symmetrical orientation of monomers. Increasing the temperature results in some of the molecules escaping temporarily from the ordered structures and accounting for the steadily increasing slope of the curve before reaching the melting temperature. After the transition, there is a dramatic change to less symmetric liquidlike structures, where some dipole reorientation would take place in the cluster as a result of the permanent intracluster motion. The size dependence of TIP4P-ice dipole moment extended to clusters with n=100 is illustrated by circles (PTMC) and squares (REMD) in Fig. 6 for T=80 K and T=280 K, respectively. According to the values found for $T_m$ in Table II, the calculations done at T=80 K correspond to solidlike structures while those at T=280 K are liquidlike clusters. In both temperature conditions, TIP4P-ice dipole moments increase substantially with size, although in the case of T=80 K they seem to reach a plateau for the larger clusters. In addition, the variation of the dipole moment versus n for small n is markedly different depending on whether the clusters behave like solid- or liquidlike particles. In Fig. 6 it is clearly shown that small and medium size solidlike water clusters exhibit dipole moments that are strongly dependent on the geometries of the dominant structures, as predicted previously in *ab initio* studies.[57,58] For example, along the simulation at T=80 K, clusters with n=8, 12, 16, and 20 explore structures that are highly symmetric, resulting in a large compensation of the overall cluster dipoles ($\langle|\mu|\rangle \approx 1$ D); for other sizes, such as n=11 and 14, the observed dipole moment is larger. For the melted clusters the sharp variation of the dipole moment with n disappears and the polarity of the particles increases uninterruptedly in the studied size range. For larger clusters ($n \geq 20$), the magnitude of the dipole moment in the liquidlike region is about 2–3 D higher than in the solidlike regimen. In the inset in Fig. 6 we represent the dipole moment per molecule as a function of n for liquidlike clusters at T=280 K. It is worth to note that this quantity rapidly decreases with the increase of cluster size, showing the expected tendency toward zero in the limit of infinitely large clusters (bulk water).

It is interesting to contrast the calculated TIP4P-ice dipole moments with the dipole moment derived from the measured effective polarizabilities of $(H_2O)_n$ clusters, $3 \leq n \leq 18$, studied by ED.[14] As mentioned before, in that work the cluster dipole is estimated by considering that the instantaneous orientations of $\mu$ on the electric field's axis occur according to a canonical distribution, well represented by the Langevin–Debye linear response theory.[59] Under these conditions, the measured effective polarizability, $\alpha_{eff}$, can be written as the sum of the electronic polarizability, $\alpha$, and a second term that represents the orientational dipolar polarization, as

$$\alpha_{eff} = \alpha + \mu^2/(3k_BT). \quad (3)$$

Dipole moments originated in the ED measurements [by use of Eq. (3)] were included for comparison in Fig. 6 (rhombuses). The data reveal a small increase of $\langle|\mu|\rangle$ with the cluster size with no sharp $\langle|\mu|\rangle$ versus n variations, which is the behavior we obtain for liquidlike structures. However, a question arises with respect to the very small $\langle|\mu|\rangle$ values derived from the ED experiment (1.3–1.8 D), which correspond more likely to the less polar solidlike structures rather than to the liquidlike forms. This might be due to the fact that the Langevin–Debye expression is not completely suitable to describe satisfactorily the cluster polarization in the field. It is probable that the clusters behave as supercooled liquid systems in the conditions of the experiment, and therefore field-induced molecular orientations do not proceed according to a canonical distribution at a well defined cluster temperature.

There are several points that are worth to mention when analyzing our results, as well as the ED experiments.[14] First of all, in our results there is no electronic polarizability effect considered. On the other hand, the ED experiments were analyzed considering the electronic polarizability of the cluster calculated by density functional theory for structures in the optimal configuration. It is hard to guess what is the average electronic polarizability of a cluster at a finite temperature and how it will affect the average total dipole moment with and without an external field. The same limitation affects the analysis of the experimental results since they

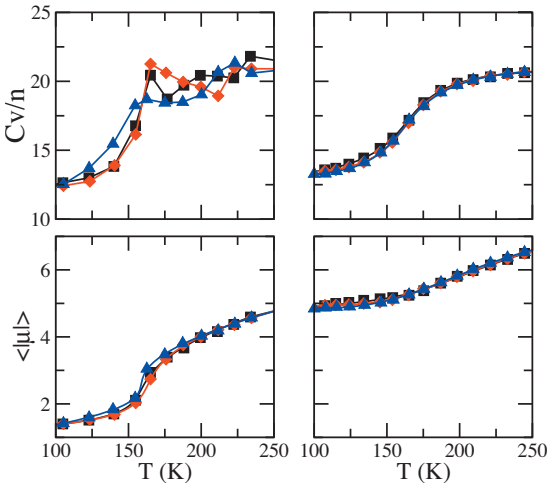


FIG. 7. Effect of external electric field on heat capacity (cal $K^{-1}$ $mol^{-1}$) and dipole moment (D) as a function of temperature for n=20 (left panels) and n=40 (right panels). Black circles, red squares, and blue diamonds correspond to electric fields of 0, 0.01, and 0.05 V/nm, respectively.

were analyzed using optimized clusters. Assuming that the main contribution to the dipole cluster moment is due to the orientational polarization, then our results suggest that the ED experiments were performed on cold clusters in the solidlike state.

Another source for the discrepancy between the calculated and ED reported dipole moments is the possibility that the external field in the ED studies modifies the cluster structure. To check this effect, we calculated the role of moderate external electric fields ($0.01-0.05$ V $nm^{-1}$) of the order of magnitude of those applied in beam ED experiments, on the transition temperature, and on the dipole moment of the clusters. Our findings, presented in Fig. 7, indicate that the presence of an external electric field of this magnitude does not affect significantly the melting temperature (n=20 and n =40) nor the average dipole moment of the cluster.

## IV. SUMMARY AND CONCLUSIONS

We have performed a computational study of water clusters, $(H_2O)_n$, with n=4–100. We have considered six different nonpolarizable water models. Among them, we give special attention to the TIP4P-ice model, which had not previously been used to model cluster systems. Using parallel tempering techniques we study the phase change of the clusters, and we monitor the cluster dipole moment as a function of temperature. As a signature for the melting transition, we used the heat capacity of the cluster. Our results show that the melting temperature of the clusters is strongly dependent on the molecular model. The sharpness of the transition (as indicated by $C_v$) also depends on the model but has a stronger dependency on the number of molecules in the cluster: Some particular cluster sizes display a very clear peak on the $C_v$ versus $T$ curve, regardless of the model. In general, the dipole moment of the cluster increases as the cluster melts, suggesting that the dipole moment could be used to distinguish between solidlike and liquidlike clusters. Finally, we considered the effect of electric fields of the same magnitude as those used in ED experiments on clusters with n=20 and n=40 molecules and found that they have a negligible effect on the cluster heat capacity and dipole moment in the whole range of temperature that we considered.

## ACKNOWLEDGMENTS

The authors acknowledge financial support from the Cooperation Program CONICET/NSF, Consejo Nacional de Investigaciones Científicas y Técnicas (Grant No. PID 5977), and Universidad of Buenos Aires (Project No. UBACyT X-050). H.R.C. and E.J.M. are members of Consejo Nacional de Investigaciones Científicas y Técnicas (CONICET). J.G.C. thanks a fellowship by CONICET. I.S. acknowledges the Raices Program from Mincyt, Argentina for the Cesar Milstein Fellowship.

[1] F. Garczarek and K. Gerwert, Nature (London) **439**, 109 (2006).
[2] I. P. Buffey, W. B. Brown, and H. A. Gebbie, Chem. Phys. Lett. **148**, 281 (1988).
[3] M. A. Zondlo, P. K. Hudson, A. J. Prenni, and M. A. Tolbert, Annu. Rev. Phys. Chem. **51**, 473 (2000).
[4] H. E. Stanley, S. V. Buldyrev, M. Canpolat, O. Mishima, M. R. Sadr-Lahijany, A. Scala, and F. W. Starr, Phys. Chem. Chem. Phys. **2**, 1551 (2000).
[5] O. Mishima and H. E. Stanley, Nature (London) **396**, 329 (1998).
[6] I. Kohl, L. Bachmann, A. Hallbrucker, E. Mayer, and T. Loerting, Phys. Chem. Chem. Phys. **7**, 3210 (2005).
[7] B. D. Kay and A. W. Castleman, J. Phys. Chem. **89**, 4867 (1985).
[8] J. D. Cruzan, L. B. Braly, K. Liu, M. G. Brown, J. G. Loeser, and R. J. Saykally, Science **271**, 59 (1996).
[9] J. K. Gregory and D. C. Clary, J. Phys. Chem. **100**, 18014 (1996).
[10] J. K. Gregory, D. C. Clary, K. Liu, M. G. Brown, and R. J. Saykally, Science **275**, 814 (1997).
[11] F. N. Keutsch and R. J. Saykally, Proc. Natl. Acad. Sci. U.S.A. **98**, 10533 (2001).
[12] K. Liu, M. G. Brown, and R. J. Saykally, J. Phys. Chem. A **101**, 8995 (1997).
[13] J. Rodriguez, D. Laria, E. J. Marceca, and D. A. Estrin, J. Chem. Phys. **110**, 9039 (1999).
[14] R. Moro, R. Rabinovitch, C. Xia, and V. V. Kresin, Phys. Rev. Lett. **97**, 123401 (2006).
[15] C. J. Burnham, J. C. Li, S. S. Xantheas, and M. Leslie, J. Chem. Phys. **110**, 4566 (1999).
[16] L. X. Dang and T. M. Chang, J. Chem. Phys. **106**, 8149 (1997).
[17] J. L. F. Abascal, E. Sanz, R. García Fernández, and C. Vega, J. Chem. Phys. **122**, 234511 (2005).
[18] J. Douady, F. Calvo, and F. Spiegelman, Eur. Phys. J. D **52**, 47 (2009).
[19] H. J. C. Berendsen, J. P. M. Postma, W. F. van Gunsteren, and J. Hermans, in *Intermolecular Forces: Proceedings of the 14th Jerusalem Symposium on Quantum Chemistry and Biochemistry*, Jerusalem, Israel, 13–16 April 1981, edited by B. Pullman (Reidel, Dordrecht, 1981).
[20] H. J. C. Berendsen, J. R. Grigera, and T. P. Straatsma, J. Phys. Chem. **91**, 6269 (1987).
[21] W. L. Jorgensen and J. D. Madura, Mol. Phys. **56**, 1381 (1985).
[22] W. L. Jorgensen, J. Chandrasekhar, J. D. Madura, R. W. Impey, and M. L. Klein, J. Chem. Phys. **79**, 926 (1983).
[23] M. W. Mahoney and W. L. Jorgensen, J. Chem. Phys. **112**, 8910 (2000).
[24] C. Vega, E. Sanz, and J. L. F. Abascal, J. Chem. Phys. **122**, 114507 (2005).
[25] E. Marinari and G. Parisi, Europhys. Lett. **19**, 451 (1992).
[26] G. T. Barkema and M. E. J. Newman, Adv. Chem. Phys. **105**, 483 (1999).
[27] E. M. Pearson, T. Halicioglu, and W. A. Tiller, Phys. Rev. A **32**, 3030 (1985).
[28] M. A. Carignano, Chem. Phys. Lett. **361**, 291 (2002).
[29] H. J. C. Berendsen, D. Vanderspoel, and R. Vandrunen, Comput. Phys. Commun. **91**, 43 (1995).
[30] E. Lindahl, B. Hess, and D. van der Spoel, J. Mol. Model. **7**, 306 (2001).
[31] A. Proykova and R. S. Berry, J. Phys. B **39**, R167 (2006).
[32] C. Vega, M. M. Conde, C. McBride, J. L. F. Abascal, E. G. Noya, R. Ramirez, and L. M. Sesé, J. Chem. Phys. **132**, 046101 (2010).

[33] B. S. González, E. G. Noya, C. Vega, and L. M. Sesé, J. Phys. Chem. B **114**, 2484 (2010).
[34] E. Asare, A-R. Musah, E. Curotto, D. L. Freeman, and J. D. Doll, J. Chem. Phys. **131**, 184508 (2009).
[35] J. Deckman and V. A. Mandelshtam, Phys. Rev. E **79**, 022101 (2009).
[36] C. J. Tsai and K. D. Jordan, J. Phys. Chem. **97**, 5208 (1993).
[37] J. M. Pedulla and K. D. Jordan, Chem. Phys. **239**, 593 (1998).
[38] A. N. Tharrington and K. D. Jordan, J. Phys. Chem. A **107**, 7380 (2003).
[39] P. Nigra, M. A. Carignano, and S. Kais, J. Chem. Phys. **115**, 2621 (2001).
[40] M. A. Carignano, A. Mohammad, and S. Kais, J. Phys. Chem. A **113**, 10886 (2009).
[41] A. V. Egorov, E. N. Brodskaya, and A. Laaksonen, Synth. React. Inorg. Met.-Org. Nano-Metal Chem. **38**, 62 (2008).
[42] A. Vegiri and S. C. Farantos, J. Chem. Phys. **98**, 4059 (1993).
[43] W. A. Adeagbo and P. Entel, Phase Transitions **77**, 63 (2004).
[44] S. V. Shevkunov and A. Vegiri, J. Mol. Struct.: THEOCHEM **574**, 27 (2001).
[45] S. V. Shevkunov and A. Vegiri, J. Mol. Struct.: THEOCHEM **593**, 19 (2002).
[46] A. V. Egorov, E. N. Brodskaya, and A. Laaksonen, Mol. Phys. **100**, 941 (2002).
[47] A. V. Egorov, E. N. Brodskaya, and A. Laaksonen, Comput. Mater. Sci. **36**, 166 (2006).
[48] G. Torchet, P. Schwartz, J. Farges, M. F. Deferaudy, and B. Raoult, J. Chem. Phys. **79**, 6196 (1983).
[49] A. Hallbrucker, E. Mayer, and G. P. Johari, J. Phys. Chem. **93**, 4986 (1989).
[50] G. P. Johari, A. Hallbrucker, and E. Mayer, Science **273**, 90 (1996).
[51] G. P. Johari, A. Hallbrucker, and E. Mayer, Nature (London) **330**, 552 (1987).
[52] G. P. Johari, A. Hallbrucker, and E. Mayer, J. Chem. Phys. **92**, 6742 (1990).
[53] I. Kohl, E. Mayer, and A. Hallbrucker, Phys. Chem. Chem. Phys. **2**, 1579 (2000).
[54] V. Velikov, S. Borick, and C. A. Angell, Science **294**, 2335 (2001).
[55] B. Bandow and B. Hartke, J. Phys. Chem. A **110**, 5809 (2006).
[56] R. G. Pereyra and M. A. Carignano, J. Phys. Chem. C **113**, 12699 (2009).
[57] H. M. Lee, S. B. Suh, J. Y. Lee, P. Tarakeshwar, and K. S. Kim, J. Chem. Phys. **112**, 9759 (2000).
[58] M. Yang, P. Senet, and C. Van Alsenoy, Int. J. Quantum Chem. **101**, 535 (2005).
[59] C. Kittel, *Introduction to Solid State Physics*, 6th ed. (Wiley, New York, 1986).